Available online at www.sciencedirect.com
SCIENCE DIRECT
Journal of Structural Biology 152 (2005) 195–203
Journal of Structural Biology
www.elsevier.com/locate/yjsbi

Crystal structure of a non-hemorrhagic fibrin(ogen)olytic metalloproteinase complexed with a novel natural tri-peptide inhibitor from venom of *Agkistrodon acutus*

Zhiyong Lou [a,b,1], Jing Hou [c,1], Xiuxia Liang [c], Jiashu Chen [c], Pengxin Qiu [c], Yiwei Liu [a,b], Ming Li [a,b], Zihe Rao [a,b,*], Guangmei Yan [c,*]

[a] *Laboratory of Structural Biology, Tsinghua University, Beijing 100084, People's Republic of China*
[b] *National Laboratory of Biomacromolecules, Institute of Biophysics, Chinese Academy of Sciences, Beijing 100101, People's Republic of China*
[c] *Department of Pharmacology, Sun Yat-Sen University of Medical Sciences, 74 Zhongshan II Road, Guangzhou 510080, People's Republic of China*

Received 26 June 2005; received in revised form 29 September 2005; accepted 30 September 2005
Available online 16 November 2005

Abstract

Thrombotic occlusive diseases pose a great threat to human health. Thrombolytic agents are in widespread use for the dissolution of arterial and venous pathologic thrombi in these kinds of diseases. Snake venom metalloproteinases (SVMPs) can act directly on fibrin/fibrinogen and are therefore potential candidates for therapeutic use against thrombotic occlusive diseases. In this study, we have determined the crystal structure of FII, a novel non-hemorrhagic SVMP isolated from Anhui *Agkistrodon acutus* snake venom by molecular replacement. The structure reveals that FII is a member of the P-I class SVMPs. The Zn^{2+} ion essential for hydrolytic activity is found in the active site and is tetrahedrally co-ordinated by three histidine residues and a water molecule. Unambiguous electron density for a tri-peptide with sequence KNL is also found located near the active site. Biochemical evidences show that the tri-peptide KNL can inhibit the enzymatic activity of FII.

Keywords: Snake venom metalloproteinase; Non-hemmorhagic; Crystal structure; Zinc binding; *Agkistrodon acutus*; Fibrin/fibrinogen; Thrombotic occlusive diseases

1. Introduction

Thrombotic occlusive diseases pose a great threat to human health. Thrombolytic agents are in widespread use for the dissolution of arterial and venous pathologic thrombi in these kinds of diseases. The clinically available thrombolytic agents, such as recombinant tissue plasminogen activator (t-PA), urokinase and streptokinase are plasminogen activators (Ouriel, 2002) and are effective in restoring blood flow in occluded arteries and veins. However, they act on the thrombus indirectly by activating plasminogen, circulating plasminogen as well as fibrin-bound plasminogen within the thrombus is activated, thus frequently lead to systemic fibrinolysis and degradation of other clotting proteins with accompanying bleeding (Ouriel, 2002). There are other disadvantages of these agents, such as a high probability of resistance to reperfusion within 90 min, and coronary reocclusion among patients with acute myocardial infarction (Collen, 1990; Rapaport, 1991), which may also be consequences of plasminogen activation. Snake venom metalloproteinases (SVMPs) can act directly on fibrin/fibrinogen without activating plasminogen, therefore they are potential candidates for therapeutic use against thrombotic occlusive diseases.

* Corresponding authors: Fax: +86 10 6277 3145 (Z. Rao), +86 20 87330758 (G. Yan).
E-mail addresses: raozh@xtal.tsinghua.edu.cn (Z. Rao), ygm@zsu.edu.cn (G. Yan).
[1] Co-first author.

1047-8477/$ - see front matter © 2005 Elsevier Inc. All rights reserved.
doi:10.1016/j.jsb.2005.09.006

SVMPs belong to the metzincin family and are a group of zinc-dependent proteolytic enzymes contained in the venom of poisonous snakes. More than 100 SVMPs have been reported to date and they are usually divided into four classes based on their sizes and the domains they contain (Bjarnasson and Fox, 1994): Class P-I, the small enzymes, contain only the protease domain; Class P-II, the medium-size enzymes, also possess a disintegrin-like domain at the carboxy terminal region; Class P-III, the most potent hemorrhagic toxins, have a cysteine-rich domain in addition to the same domains of P-II; Class P-IV has a fourth lectin-like domain following the cysteine-rich domain. SVMPs can act locally and/or systemically on the blood system, resulting in severe bleeding by interfering with the blood coagulation and haemostatic plug formation (Andrews and Berndt, 2000; Kamigut et al., 1996) or by degrading the vascular basement membrane or extracellular matrix components (Gutierrez and Rucavado, 2000).

Following the first reported crystal structure of adamalysin II, a P-I class SVMP from the Eastern Diamond-backed Rattlesnake *Crotalus adamanteus* (Gomis-Ruth et al., 1994), the three-dimensional structures of several P-I class SVMPs have been reported by X-ray crystallography (Gong et al., 1998; Huang et al., 2002a; Kumasaka et al., 1996; Watanabe et al., 2003; Zhu et al., 1999). These enzymes share the same overall topology, especially in the zinc-binding environment, for a hydrolytic reaction. The elucidation of the structures of these SVMPs will help determine their structure–function relationships, and thus their potential pharmacological use.

A novel SVMP was isolated from Anhui *Agkistrodon acutus* snake venom in our laboratory and named FII (Liang et al., 2001). Like other SVMPs of the P-I class, such as fibrolase from *Agkistrodon contortrix contortrix* (Randolph et al., 1992), atroxase from *Crotalus atrox* (Tu et al., 1996), lebetase from *Vipera lebetina* (Siigur et al., 1998), neuwiedase from *Bothrops neuwied* (Rodrigues et al., 2000) and BaPl from *Bothrops asper* (Gutierrez et al., 1995), FII can directly degrade the α- and β-chains of fibrin and fibrinogen in vitro (Chen et al., 1993; Liang et al., 2001) and dissolve thrombus effectively in vivo (Chen et al., 1998), but have no influence on tissue-type plasminogen activator and plasminogen activator inhibitor-1 activities in plasma (Liang et al., 2001). These results imply that snake venom metalloproteinase FII has potential therapeutic use in dissolving thrombi.

To better understand the proteolytic mechanism of this enzyme, here we report the crystal structure of FII by X-ray crystallography.

2. Materials and methods

2.1. Purification of FII

The lyophilized powder of *A. acutus* venom was purchased from Qimen snake farm (Anhui, China). The isolation procedures were performed at 4 °C as described elsewhere (Chen et al., 1993; Liang et al., 2001) with some modifications. In short, crude venom dissolved in 0.05 M ammonium acetate (pH 8.0) was applied to a DEAE-Sephadex A-50 column (3.0 × 80 cm, Pharmacia) previously equilibrated with 0.05 M ammonium acetate (pH 8.0). Fractions were eluted with a linear gradient from 0.05 M ammonium acetate (pH 8.0) to 1 M ammonium acetate (pH 5.0). The second fraction eluted by ion-exchange chromatography was collected, concentrated and then applied to a Sephadex G-50 column (1.1 × 100 cm, Pharmacia) pre-equilibrated with 0.01 M ammonium acetate (pH 8.0). The first fraction eluted by gel filtration was collected, concentrated and applied again to a Sephadex G-50 column. The first fraction eluted by the final gel filtration was collected, dialyzed against distilled water and lyophilized. After the above isolation steps, 23 mg of FII was obtained from 2 g of crude venom. The fibrinolytic activity measured by using a modified fibrin plate technique (Astrup and Mullertz, 1952) rose from $60 \pm 16\,mm^2/\mu g$ protein after the ion-exchange chromatography to $90 \pm 12\,mm^2/\mu g$ protein after the final gel filtration.

The lyophilized FII powder was dissolved in 10 mM Tris–HCl (pH 8.0), 0.15 M NaCl, applied to a Superdex G75 gel filtration column (Pharmacia), and eluted with the same buffer at a flow rate of 0.5 ml/min. The first fraction was collected, dialyzed against pure water and concentrated to about 10 mg/ml.

2.2. Determination of protein concentration

Protein concentration was determined using a bicinchoninic acid (BCA) based protein assay kit (Pierce) with bovine serum albumin (BSA, Sigma) as standard.

2.3. Determination of molecular weight

Sodium dodecyl sulfate–polyacrylamide gel electrophoresis (SDS–PAGE) was performed according to the method of Laemmli (1970). Molecular weight standards were MBPb-galactosidase (175 kDa), MBP-paramyosin (83 kDa), glutamic dehydrogenase (62 kDa), aldolase (47.5 kDa), triosephosphate isomerase (32.5 kDa), β-lactoglobulin A (25 kDa), lysozyme (16.5 kDa), and aprotin in (6.5 kDa).

2.4. Crystallization of FII

The freshly prepared protein was crystallized by the hanging drop vapor diffusion method at 291 K. The crystallization conditions were screened using Crystal Screen Kits I and II (Hampton Research), based on the sparse-matrix method (Jancarik and Kim, 1991). One microliter of protein solution was mixed with 1 μl of reservoir solution and equilibrated against 200 μl of reservoir solution. Fine shaped crystals grown in Kit I-38 condition (1.4 M trisodium citrate, 0.1 M Na Hepes, pH 7.5) appeared at the

second day and reached their final volumes of about $50 \times 50 \times 200$ μm in 4 weeks without any optimization.

2.5. Data collection, processing and structure determination

Data for the wild-type FII crystal were collected on a Rigaku R-AXIS IV++ image plate with a Rigaku rotating anode home X-ray generator at 40 kV and 20 mA ($\lambda = 1.5418$ Å). The crystals were soaked for several minutes in the reservoir solution supplemented with 20% glycerol as a cryoprotectant and then flash cooled directly in liquid nitrogen. All data were collected at 100 K (Table 1). Data were processed and scaled using the program HKL2000 (Otwinowski and Minor, 1997).

2.6. Structure determination and refinement

The structure of wild-type FII was determined by molecular replacement using the structure of adamalysin II (Gomis-Ruth, 1993) as a search model in CNS (Brunger et al., 1998). One clear solution for both the rotation and translation functions indicated the presence of only one molecule in the asymmetric unit. Residues that differ between FII and adamalysin II were replaced, and geometric adjustments were made in O (Jones and Kjeldgaard, 1997) under the guidance of $F_o - F_c$ and $2F_o - F_c$ electron density maps. After the refinement of the model was done using simulated annealing, energy minimization, restrained individual B factor, and adding water molecules, the R-factor and R_{free} dropped from 40.2% and 42.8% to 21.7% and 23.4% between 50 and 1.9 Å. Throughout refinement, the agreement between the model and the observed data was monitored by calculating R_{free} based on 5% of the reflections. The stereochemical quality of the refined structures was checked with the program PROCHECK (Laskowski et al., 1993). The atomic coordinates of the FII crystal structure have been deposited in the Protein Data Bank with accession number 1YP1.

Table 1
Data collection and refinement statistics

Parameters	Wild-type FII
Data collection	
Cell parameters (Å)	$a = b = 80.6$, $c = 66.8$
Space group	$P3_12_1$
Resolution (Å)	50.0–1.9
Total No. of reflections	183 192
Unique reflections	23 498
Completeness (%)	99.5 (100.0)
Average $I/\sigma(I)$	21.2 (7.1)
R_{merge} [a]	7.1 (45.5)
Refinement	
Refinement data No. of reflections (>0 $\sigma(F)$)	19 624
$R_{working}$ [b]	21.7
R_{free} (5% data)	23.4
r.m.s.d. bond distance (Å)	0.012
r.m.s.d. bond angle (°)	1.9
Average B value/No. of atoms all nonhydrogen atoms	33.3
Solvent atoms	134
Ramachandran plot (excluding prolines and glycines)	
Residues in most favored regions	165 (91.2%)
Residues in additional allowed regions	15 (8.3%)
Residues in generously allowed regions	1 (Cys117, 0.6%)

Numbers in parentheses correspond to the highest resolution shell.
All refinement and calculation of R factor were performed in CNS using all reflections.
[a] $R_{merge} = \sum_{hkl}\sum_i |I(hkl)_i - \langle I(hkl)\rangle| / \sum_{hkl}\sum_i I(hkl)_i$.
[b] $R_{working} = \sum_{hkl} |F(hkl)_{obs} - \langle F(hkl)_{calc}\rangle| / \sum_{hkl} F(hkl)_{obs}$.

2.7. Azocaseinolytic activity assay of FII and its inhibition by tri-peptide KNL

One milligram lyophilized FII powder was dissolved in 200 μl distilled water. One microliters of this solution was drawn, dialyzed against distilled water and then concentrated to a final volume of about 100 μl. Both the dialyzed sample and un-dialyzed sample were carefully adjusted to a protein concentration of 1 mg/ml.

One hundred microliter reaction mixture, containing 1 μg enzyme with or without indicated concentrations of synthetic tri-peptide KNL (Shanghai Sangon) and 100 μg azocasein (Sigma) in 50 mmol/L Tris–HCl, pH 8.0, was incubated at 37 °C for 30 min, then 100 μl of 10% trichloracetic acid was added to the mixture to terminate the proteolysis reaction. The reaction mixture was allowed to stand at room temperature for 30 min and then centrifuged at 10,000 rpm, 4 °C for 10 min. The supernatant was drawn to measure the absorbance at 390 nm on a Smartspect 3000 spectrophotometer (Bio-Rad). The caseinolytic activity of FII was reflected by absorbance at 390 nm. The relative enzymatic activity with the addition of a tri-peptide with sequence KNL was estimated by comparison of the absorbance at 390 nm with that of control (without addition of the tri-peptide).

3. Results and discussion

3.1. Crystallographic sequence and the overall structure

The purified FII showed a molecular weight of approximately 26 kDa from SDS–PAGE. However, the current sequence of FII, as indicated by the experimental electron density map, contains only 199 amino acid residues with a calculated molecular weight of 21.6 kDa (ExPasy ProtParam Tool). The difference between the two molecular weights might be due to the unseen terminal residues of the protein in the electron density map. It should be noted that our attempts to perform chemical sequencing of FII were unsuccessful and the sequence could only be determined from the experimental electron density map, as in the previous case of the SVMP Acutolysin A reported by Gong et al. (1998).

Like the other members of the P-I class SVMPs (PDB codes: 1BSW, 1HTD, 1IAG 1KUF, 1ND1, 1QUA), an FII

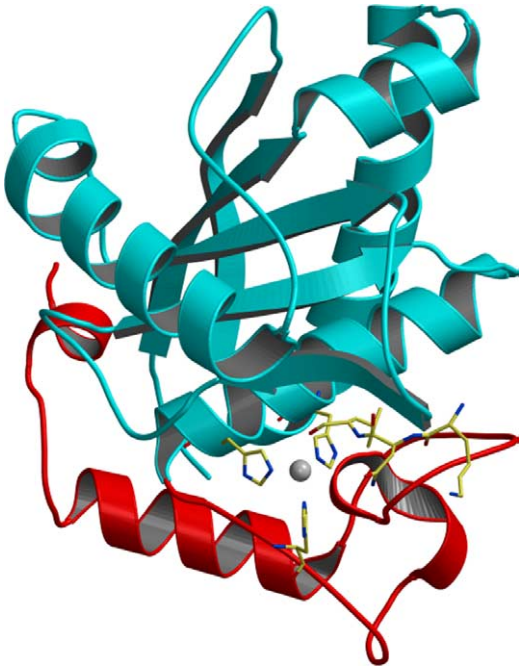

Fig. 1. The overall structure of FII. The cyan part is the N terminal domain which contains four parallel and one anti-parallel β-sheets and four α-helixes; the red part is the C terminal domain which contains long α-helix and a complicated Met turn. The grey sphere represents a Zn^{2+} ion; the three zinc-chelating histidines and KNL tri-peptide inhibitor are shown in ball-and-stick mode.

molecule has two subdomains (Fig. 1) and two highly conserved characteristic sequences, namely $H_{142}E_{143}XXH_{146}XXGXXH_{152}$ and $C_{163}I_{164}M_{165}$. The N-terminal domain is the larger of the two subdomains (3/4 of the full-length protein) and is a classic α/β structure. There are four parallel and one anti-parallel β-sheets, which are surrounded by four α-helixes. The smaller C-terminal domain (residues 149–200) contains a long α-helix and a complicated Met-turn. The Met-turn has been described previously for several SVMP structures (Gomis-Ruth, 1993; Gomis-Ruth et al., 1994; Gong et al., 1998). The Zn^{2+} ion, which is necessary for the hydrolytic activity, lies in the gap between the two domains and is chelated in a tetrahedral manner by the Nε2 nitrogen atoms of three histidine residues in the highly conserved HEXXHXXGXXH sequence motif and three water molecules. We also observe unambiguous electron density around the active site for a tri-peptide with the amino acid sequence of Lys-Asn-Leu (KNL).

Although most SVMPs can cause severe bleeding, some SVMPs, primarily those belonging to the P-I class, are devoid of hemorrhagic activity (Randolph et al., 1992; Rodrigues et al., 2000). The structural basis of this observation is not clear, although some studies comparing sequences of hemorrhagic and non-hemorrhagic metalloproteinases have identified residues which may be required to exert this effect (Bolger et al., 2001; Gasmi et al., 2000). Our previous work had shown that intravenous injection of FII to Wistar rats at a dosage of 5 mg/kg did not cause hemorrhaging in heart, liver and lung tissue (Liang et al., 2001). However, we did not identify any special residues when comparing the amino acid sequences of FII with the other seven non-hemorrhagic and eight hemorrhagic SVMPs (Fig. 2).

Recent evidences have proposed that post-transcriptional modification, such as glycosylation (Garcia et al., 2004), and some molecular characteristics, such as molecular surface properties (Ramos and Selistre-de-Araujo, 2004) may be related to the hemorrhagic activity of SVMPs. Deglycosylated forms of two hemorrhagic SVMPs, Jararhagin and ACLH, did not show any hemorrhagic activity but preserved their proteolytic activities toward fibrinogen and fibronectin, suggesting that presence of glycan in the protein molecule may contribute to the substrate specificity (Garcia et al., 2004). FII is not glycosylated although it has a potential glycosylation site (NCSY). Whether the glycosylation status and molecular surface feature of FII contribute to its non-hemorrhagic activity or not remains to be clarified by further research.

3.2. The zinc-ion binding environment

Each member of the metzincins has a Zn^{2+} ion in the active site that is essential for their hydrolytic activity. The structures of metzincins determined to date show that the Zn^{2+} ion is usually chelated by the Nε2 nitrogen atoms of three histidine residues in the highly conserved sequence HEXXHXXGXXH, together with one or two water molecules. It has been shown that in some other SVMPs, such as TM-3 (PDB codes: 1KUF, 1KUG, 1KUI, 1KUK) from the venom of *Taiwan habu*, and Acutolysin A (PDB code: 1BUD) from the venom of *Agkistrodon acutus*, etc., only have one or two water molecules co-ordinating the Zn^{2+} ion. The crystal structure of FII features one co-ordinating water molecule (Watl) clearly defined by the electron density map, and located at a distance of 2.29 Å from the zinc ion. This suggests that the zinc ion is tetrahedrally chelated in the structure of FII (Fig. 3).

3.3. The disulfide bonds

The electron density map indicates that there are three disulfide bonds in a single molecule, formed between Cys117–Cys196, Cys158–Cys180 and Cys160–Cys163. FII is therefore classified as a three-disulfide SVMP according to the classification criteria of Gong et al. (1998), similar to most other SVMPs. Among these three connections, Cys117–Cys196 is a highly conserved disulfide bond found in almost every member of the SVMP family. Cys158–Cys180 lies on the outside turn of all structures of SVMPs, and the environment can be changed easily due to crystal packing, pH, etc., thus causing the conformation of this connection to vary greatly between FII and other SVMPs (Fig. 4). This may explain why, despite the high sequence homology between FII and TM-3 (43% identity in 197 residues), we still cannot see this disulfide bond and even the whole turn clearly when using 1KUG as the initial search model for molecular replacement.

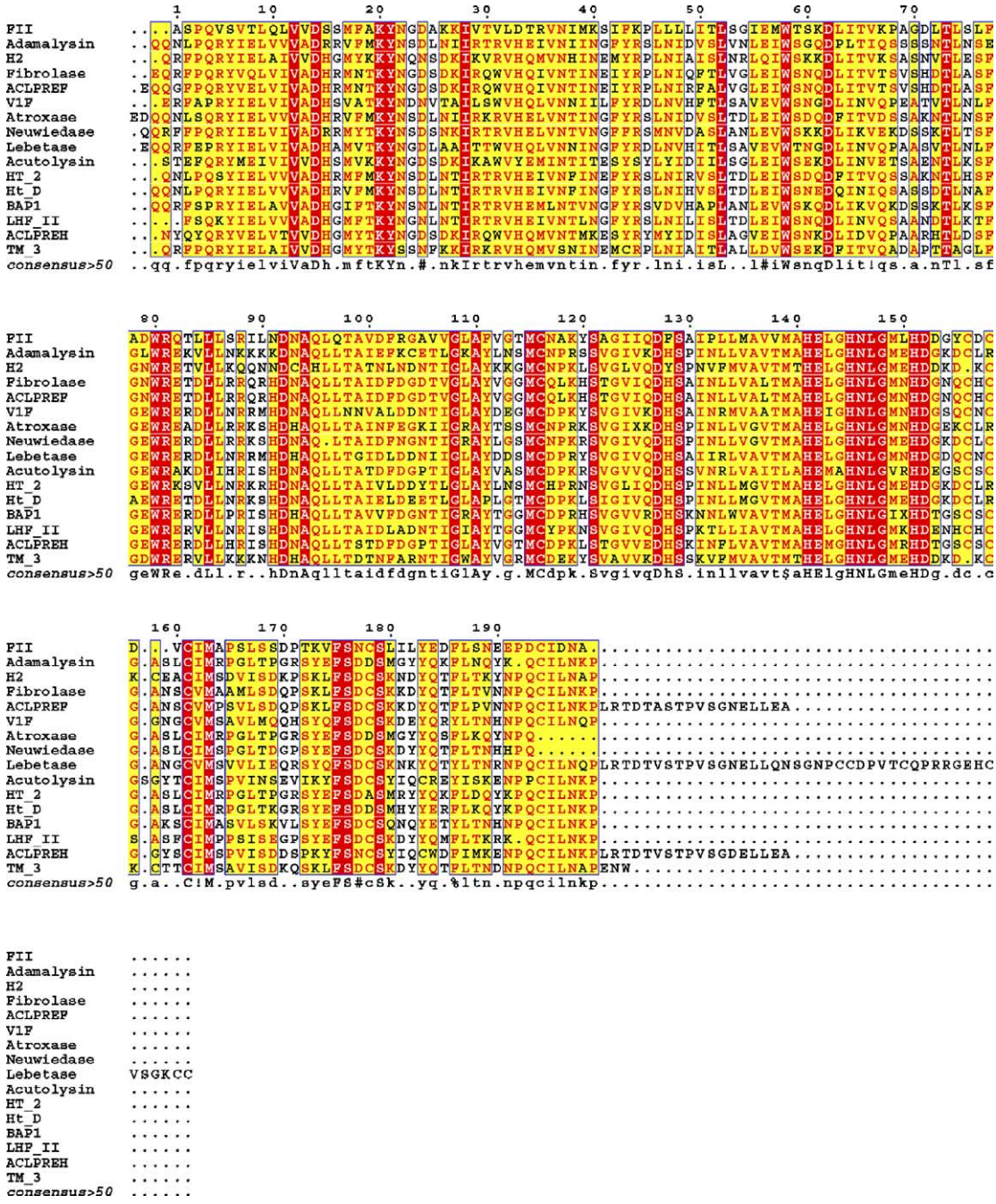

Fig. 2. Multiple sequence alignment of the amino acid sequences of FII with the other seven non-hemorrhagic and eight hemorrhagic SVMPs. Non-hemorrhagic SVMPs: Adamalysin II from *Crotalus adamanteus* (Gomis-Ruth, 1993); H2 from *Trimeresurus flavoviridis* (Kumasaka et al., 1996); Fibrolase from *Agkistrodon contortrix contortrix* (Randolph et al., 1992); ACLPREF from *Agkistrodon contortrix laticinctus* (Selistre de Araujo and Ownby, 1995). VlF from *Vipera lebetina* (Gasmi et al., 2000); Atroxase from *Crotalus Atrox* (Tu et al., 1996); Neuwiedase from *Bothrops neuwiedi* (Rodrigues et al., 2000). Hemorrhagic SVMPs: Lebetase from *Vipera lebetina* (Siigur et al., 1998); Acutolysin A from *A. acutus* (Gong et al., 1998); HT-2 from *Crotalus ruber rubber* (Takeya et al., 1990); atrolysin C from *Crotalus atrox* (Zhang et al., 1994); BaP1 from *Bothrops asper* (Watanabe et al., 2003); LHFII from *Lachesis muta muta* (Sanchez et al., 1991); ACLPREH from *Agkistrodon contortrix laticinctus* (Selistre de Araujo and Ownby, 1995); TM-3 from Taiwan Habu (Huang et al., 2002a,b). Sequences were aligned using CLUSTAL W (1.82).

3.4. The tri-peptide inhibitor binding and its effects on the activity of FII

Snakes protect themselves from the effects of their own toxic venom components in a variety of ways: (1) many metalloproteinases are synthesized and stored in the venom gland as inactive zymogens, with a conserved thiol group in the prosequence PKMCGV blocking the active site by binding to the zinc ion. After secretion from the gland, the proteolytic processing converts the zymogen to the active enzyme by removing this thiol group (Grams et al., 1993). (2) Some snake sera contain glycoproteins that form a complex with

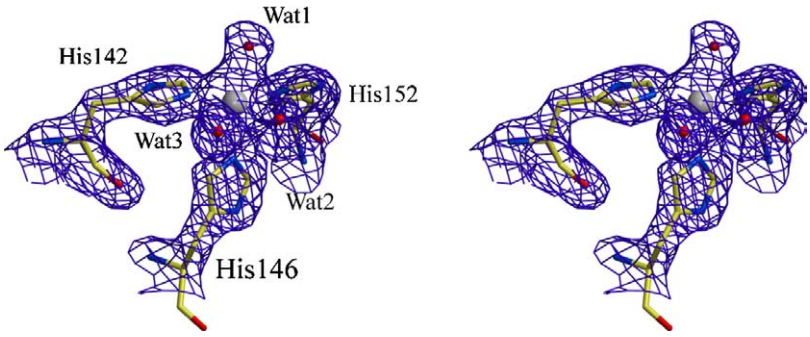

Fig. 3. Stereo view of the zinc binding environment. The Zn^{2+} ion is tetrahedrally bound by His142, His146, His 152 and water molecules Wat1.

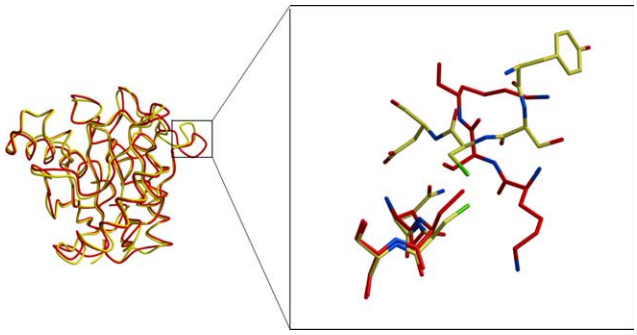

Fig. 4. Comparison of FII with TM-3. Left: The overall structure of FII is shown in yellow; the overall structure of TM-3 (PDB code: 1KUG) is shown in red. Right: Comparison of the third disulfide bridge. The third disulfide bridge environment of FII is shown in yellow; the third disulfide bridge environment of TM-3 (PDB code: 1KUG) is shown in red.

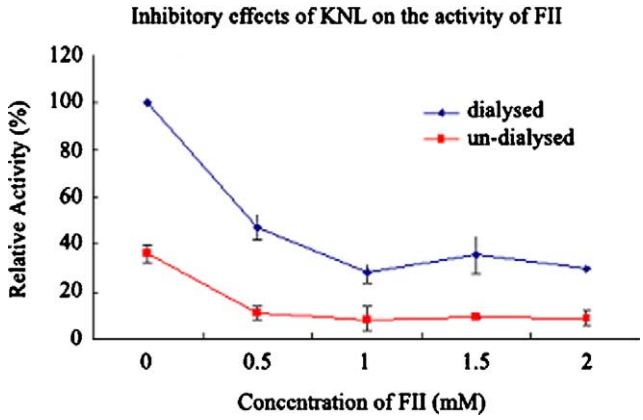

Fig. 5. Inhibitory effects of tri-peptide KNL on activity of FII toward azocasein. Points show the mean of three replicates ±1 standard deviation. The red line shows the activity of undialysed FII. The blue line shows the activity of dialysed FII.

venom hemorrhagic proteinases and thereby neutralize their activity (Weissenberg et al., 1991). (3) Many venoms contain high concentrations of citrate that inhibit enzymes by metal–ion chelation (Francis et al., 1992,). (4) Inhibitory peptides present in venom allow snakes to be protected from their own toxic proteinases and inhibit hydrolysis of venom proteins during storage in the venom gland (Francis and Kaiser, 1993). Upon dilution, such as when venom is injected into prey, citrate and peptide inhibitors dissociate from the proteinases and allow their activation.

Several snake venom metalloproteinase inhibitory tri-peptides have been isolated and characterized, such as pEQW and pENW from the venoms of *Agkistrodon halys blomhoffii*, *Crotalus adamanteus*, *Bothrops Jararaca*, *Tri meresurus flavoviridis* (Kato et al., 1966) and other kinds of rattle snakes (Munekiyo and Mackessy, 2005); pEWK, pEEW and pENW from the venoms of *Trimeresurus mucrosquamatus* and *Trimeresurus gramineus* (Lo, 1972); and pEKS from the venom of *A. h. blomhoffii* (Okada et al., 1974). All of these peptides have a pyro-glutamate at the N-terminal. The crystal structures of TM-3 with the three tri-peptides pENW (PDB code: 1KUG), pEQW (PDB code: 1KUI), and pEKW (PDB code: 1KUK) have been determined (Huang et al., 2002a,b).

In the crystal structure of FII, a tri-peptide with sequence KNL is found to bind to the active site of the enzyme (Fig. 5B). This peptide is quite different from other previously reported inhibitory peptides. We assume that this tri-peptide acts as an inhibitor of FII, since the dialyzed FII showed about three times higher activity towards azocasein than the un-dialyzed enzyme when no KNL was added. Furthermore, addition of KNL inhibited the activity of the dialyzed enzyme (Fig. 5). This fact indicates that KNL is reversibly bound to FII. Addition of KNL to the un-dialysed sample also inhibited the enzymatic activity (Fig. 5) and may be due to the dialysis step during the purification process. However, within the concentration range used in this study, the enzymatic activity of both the dialyzed and un-dialyzed FII could not be completely inhibited.

The inhibitor KNL inserts between the "bulged" segment and the S1-wall forming segment under formation of a mixed parallel–antiparallel three-stranded β-sheet. Each residue is clearly defined by unambiguous electron density, including the side chain of Lys-Bl (Fig. 6A).

3.4.1. The P3 (binding to S1 site) Leu-B3 residue of the inhibitor

The S1 site is occupied by Leu-B3, which is different from residues in other reported tri-peptides. The plane formed by the Cβ, Cδ1 and Cδ2 atoms of Leu-B3 is stacked against the imidazole ring of His 142 with a similar conformation to the equivalent Trp residue found in the structures of tri-peptide

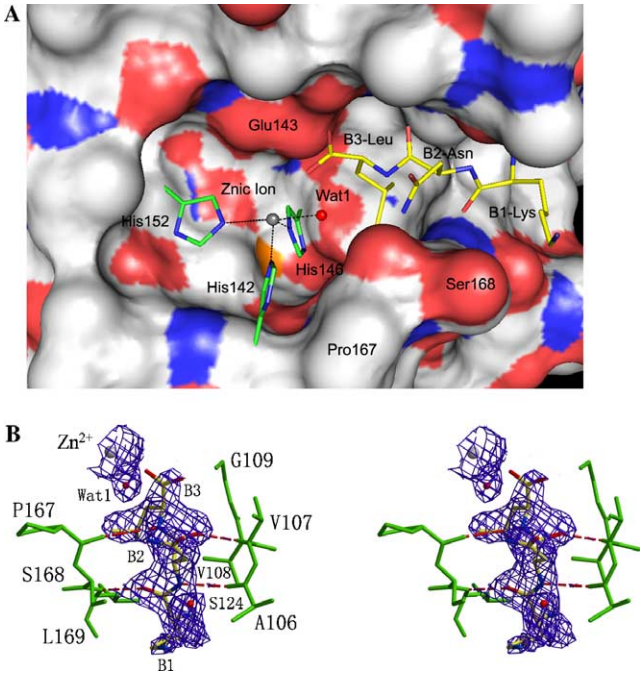

Fig. 6. (A) Overall inhibitor binding environment. (B) Stereo view of the inhibitor binding pocket. The main chain residues of FII are shown in green; the residues of the inhibitor are shown in yellow. The inhibitor is shown covered by the $2F_o - F_c$ electron density map (contoured at 1.0 σ level). The grey sphere represents the Zn^{2+} ion; red spheres represent water molecules.

inhibitors of TM-3 (Huang et al., 2002a,b). The average distance between the imidazole ring and B3 sidechain plane is 3.72 Å, which is a good hydrophobic contact. In addition, the distance from the N atom of Leu-B3 to the O atom of Prol 67 is 3.94 Å, which is far from an ideal hydrogen bond but can still co-operate in anchoring the inhibitor into the active site. According to the structure of FII, the S1 pocket is not fulfilled by the Leu-B3 side chain. There are still three ordered water molecules occupying this pocket upon binding of a Leu-containing inhibitor, which is similar to the structure of adamalysin II (Cirilli et al., 1997). The carboxylate oxygen atom of Leu-B3 is located close to the Oεl and Oε2 atoms of the probably protonated Glu l43, with respective distances of 3.62 and 2.83 Å. Glu l43 has been considered to play the role of the general base in the commonly accepted mechanism by which means zinc proteases cleave their protein substrates (Grams et al., 1996; Kester and Matthews, 1977). This fact further suggests that the KNL tri-peptide might be an inhibitor of FII.

3.4.2. The P2 Asn-B2 residue of the inhibitor

As shown in Fig. 5A, the Asn-B2 residue of the inhibitor is stabilized in the S2 site of FII by two hydrogen bonds: (a) The N atom of Asn-B2 is hydrogen-bonded to the carbonyl oxygen of Ala106 with a distance of 2.72 Å. (b) The carbonyl oxygen of Asn-B2 is hydrogen-bonded to the N-terminal nitrogen of Val108 with a distance of 2.71 Å. Some other structures of SVMP containing inhibitors feature an additional hydrogen bond between the side chains of Asn-B2 and the residue in position 106. However, in the structure of FII, the residue in position 106 is alanine, and hence there is no counterpart to this hydrogen bond in our structure.

3.4.3. The P1 Lys-B1 residue of the inhibitor

The P1 residue of this inhibitor is completely different from the other inhibitors reported previously. In the other SVMP structures containing inhibitors, P1 residues usually contain a pyro-group. However, in our structure, there is a lysine residue located in the P1 position. The carbonyl oxygen of Lys-Bl forms a hydrogen bond with the N-terminal nitrogen of Leu l70 with a distance of 2.90 Å. This contact helps to stabilize Lys-Bl in its position. An additional water molecule, Wat 124, is hydrogen-bonded to the Nz atom of Lys-Bl.

4. Conclusions

We report the 1.9 Å high-resolution crystal structure of FII with a novel endogenous tripeptide inhibitor with sequence KNL. From the unambiguous electron density map, we determined the sequence of this inhibitor, and performed biological assays to show that this tri-peptide has an inhibitory effect on FII. The inhibitor exhibits classical binding to FII, similar to other SVMP-inhibitor complexes: (a) the side chain of Leu-B3 inserts into the S1 pocket; (b) the second residue Asn-B2 is stabilized in the S2 pocket by two good hydrogen bonds; (c) the third residue, Lys-Bl, which is quite different from the classical SVMPs, is stabilized by ideal hydrogen bonds. FII has a zinc binding site, in common with other SVMPs. In addition to the three conserved His chelating groups, the Zn^{2+} is also co-ordinated by water molecules (Wat1). To the best of our knowledge, FII is the first non-hemorrhagic SVMP structure to be determined and we propose that this would account for differences in the zinc binding and inhibitor of FII and other SVMPs. Further work is underway to confirm our hypotheses.

Acknowledgments

G.Y. was supported by a grant from The Science and Technology Program of Guangdong Province, China (No. 2003A10905). Z.R. was supported by grants from Projects “863” (No. 2002BA711A12) and “973” (No. G1999075602) of the Ministry of Science and Technology, China.

References

Andrews, R.K., Berndt, M.C., 2000. Snake venom modulators of platelet adhesion receptors and their ligands. Toxicon 38, 775–791.

Astrup, T., Mullertz, S., 1952. The fibrin plate method for estimating of fibrinolytic activity. Arch. Biochem. Biophys. 40, 346–351.

Bjarnasson, J.B., Fox, J.W., 1994. Hemorrhagic metalloproteinases from snake venoms. Pharmacol. Ther. 62, 325–372.

Bolger, M.B., Swenson, S., Markland, F.S., 2001. Three-dimensional structure of fibrolase, the fibrinolytic enzyme from southern copperhead venom, modeled from the X-ray structure of adamolysin II and atrolysin C. AAPS PharmSci. 3, E16.

Brunger, A.T, Adams, P.D., Clore, G.M., et al., 1998. Crystallography and NMR system: a new software suite for macromolecular structure determination. Acta Crystallogr. D 54, 905–921.

Chen, J.S., Liang, L.G, Sun, J.J., 1993. The pharmacology characterizations of fibrinolytic fraction II from five-pace snake venom. Chin. Pharmacol. Bull. 9, 22–25.

Chen, J.S., Yu, L.P., Liang, X.X., Liang, L.G, 1998. Thrombolysis with *agkistrodon acutus* venom fraction II in a rat model of carotid thrombosis. Chin. Pharmacol. Bull. 14, 462–463.

Cirilli, M., Gallina, C., Gavuzzo, E., Giordano, C., Gomis-Ruth, F.X., Gorini, B., Kress, L.F., Mazza, F., Paglialunga Paradisi, M., Pochetti, G., Politi, V., 1997. 2A X-ray structure ofadamalysin II complexed with a peptide phosphonate inhibitor adopting a retro-binding mode. FEBS Lett. 418, 319–322.

Collen, D., 1990. Coronary thrombolysis: streptokinase or recombinant tissue-type plasminogen activator. Ann. Intern. Med. 112, 529–538.

Francis, B., Seebart, C., Kaiser II, 1992. Citrate is an endogeneous inhibitor of snake venom enzymes by metal-ion chelation. Toxicon 30, 1239–1246.

Francis, B., Kaiser II, 1993. Inhibition of metalloproteinases in Bothrops Asper venom by endogeneous peptides. Toxicon 31, 889–899.

Freitas, M.A., Geno, P.W., Sumner, L.W., Cooke, M.E., Hudiberg, S., Ownby, C.L., Kaiser II, Odell, GV., 1992. Citrate is a major component of snake venoms. Toxicon 30, 461–464.

Garcia, L.T., Parreiras e Silva, L.T., Ramos, O.H.P., Carmona, A.K, Bersanetti, P.A., Selistre-de-Araujo, H.S., 2004. The effect of post-translational modifications on the hemorrhagic activity of snake venom metalloproteinases. Comp. Biochem. Physiol. C 138, 23–32.

Gasmi, A., Srairi, N., Karoui, H., El Ayeb, M., 2000. Amino acid sequence of V1F: identification in the C-terminal domain of residues common to non-hemorrhagic metalloproteinases from snake venoms. Biochim. Biophys. Acta 1481, 209–212.

Gomis-Ruth, F.X., Kress, L.F., Kellermann, J., et al., 1994. Refined 2.0A X-ray crystal structure of the snake venom zinc-endopeptidase adamalysin II: primary and tertiary structure determination, refinement, molecular structure and comparison with astacin, collagenase and thermolysin. J. Mol. Biol. 239, 513–544.

Gomis-Ruth, F.X., 1993. First structure of a snake venom metalloproteinase: a prototype for matrix metalloproteinases/collagenases. EMBO J. 12, 4151–4157.

Grams, F., Dive, V., Yiotakis, A., Yiallouros, I., Vassiliou, S., Zwilling, R., Bode, W., Stocker, W., 1996. Structure of astacin with a transition-state analogue inhibitor. Nat. Struct. Biol. 3, 671.

Grams, F., Huber, R., Kress, L.F., Moroder, L., Bode, W., 1993. Activation of snake venom metalloproteinases by a cysteine switch-like mechanism. FEBS Lett. 335, 76–80.

Gutierrez, J.M., Romero, M., Diaz, C., Borkow, G., Ovadia, M., 1995. Isolation and characterization of a metalloproteinase with weak hemorrhagic activity from the venom of the snake *Bothrops asper* (terciopelo). Toxicon 33, 19–29.

Gutierrez, J.M., Rucavado, A., 2000. Snake venom metalloproteinases: their role in the pathogenesis of local tissue damage. Biochimie 82, 841–850.

Gong, W., Zhu, X., Liu, S., Teng, M., Niu, L., 1998. Crystal structures of acutolysin A, a three-disulfide hemorrhagic zinc metalloproteinase from the snake venom of *Agkistrodon acutus*. J. Mol. Biol. 283, 657–668.

Huang, K.F., Chiou, S.H, Ko, T.P., Wang, A.H.J., 2002a. The 1.35 A structure of cadmium-substituted Tm-3, a snake-venom metalloproteinase from *Taiwan habu*: elucidation of a TNF-alpha-converting enzyme-like active-site structure with a distorted octahedral geometry of cadmium. Acta Crystallogr. D 58, 1118.

Huang, K.F., Chiou, S.H, Ko, T.P., Wang, A.H.J., 2002b. Determinants of the inhibition of a *Taiwan habu* venom metalloproteinase by its endogenous inhibitors revealed by X-ray crystallography and synthetic inhibitor analogues. Eur. J. Biochem. 269, 3047–3056.

Jones, T.A., Kjeldgaard, M., 1997. Electron-density map interpretation. Methods Enzymol. 277, 173–208.

Jancarik, J., Kim, S.H., 1991. Sparse matrix sampling: a screening method for crystallization of proteins. J. Appl. Cryst. 24, 409–411.

Kamigut, A.S., Hay, C.R., Theakston, R.D., Zuzel, M., 1996. Insights into the mechanism of haemorrhage caused by snake venom metalloproteinases. Toxicon 34, 627–642.

Kato, H., Iwanaga, S., Suzuki, T., 1966. The isolation and amino acid sequences of new pyroglutamylpeptides from snake venoms. Experientia 22, 49–50.

Kumasaka, T., Yamamoto, M., Moriyama, H., Tanaka, N., Sato, M., Katsube, Y., Yamakawa, Y., Omori- Satoh, T., Iwanaga, S., Ueki, T., 1996. Crystal structure of H2-proteinase from the venom of *Trimeresurus flavoviridis*. J. Biochem. 119, 49–57.

Kester, W.R., Matthews, B.W., 1977. Comparison of the structures of carboxypeptidase A and thermolysin. J. Biol. Chem. 252, 7704–7710.

Laskowski, R.A., MacArthur, M.W., Moss, D.S., Thornton, J.M., 1993. PROCHECK: program to check the stereochemical quality of protein structures. J. Appl. Crystallogr. 26, 283–291.

Laemmli, U.K., 1970. Cleavage of structural proteins during the assembly of the head of bacteriophage T4. Nature 227, 680–685.

Liang, X.X., Chen, J.S., Zhou, Y.N., Qiu, P.X., Yan, G.M, 2001. Purification and biochemical characterization of FIIa, a fibrinolytic enzyme from *Agkistrodon acutus* venom. Toxicon 39, 1133–1139.

Lo, T.P., 1972. Chemical studies of Formosan snake venoms. J. Chin. Biochem. Soc. 1, 39–46.

Munekiyo, S.M., Mackessy, S.P., 2005. Presence of peptide inhibitors in rattlesnake venoms and their effects on endogenous metalloproteases. Toxicon 45, 255–263.

Okada, K., Nagai, S., Kato, H., 1974. A new pyroglutamylpeptide (Pyr-Lys-Ser) isolated from the venom of *Agkistrodon halys blomhoffii*. Experientia 30, 459–460.

Otwinowski, Z., Minor, W., 1997. Methods Enzymol. 267, 307–326.

Ouriel, K., 2002. Comparison of safety and efficacy of the various thrombolytic agents. Rev. Cardiovasc. Med. 3 (Suppl. 2), S17–S24.

Ramos, O.H.P., Selistre-de-Araujo, H.S., 2004. Comparative analysis of the catalytic domain of hemorrhagic and non-hemorrhagic snake venom metallopeptidases using bioinformatic tools. Toxicon 44, 529–538.

Randolph, A., Chamberlain, S.H., Chu, H.L., Retzios, A.D., Markland, F.S., Masiarz, F.R., 1992. Amino acid sequence of fibrolase, a direct-acting fibrinolytic enzyme from *Agkistrodon contortrix contortrix* venom. Protein Sci. 1, 590–600.

Rapaport, E., 1991. Thrombolysis, anticoagulation, and re-occlusion. Am. J. Cardiol. 68, 17E–22E.

Rodrigues, V.M., Soares, A.M., Guerra-Sa, R., Rodrigues, V., Fontes, M.R., Giglio, J.R., 2000. Structural and functional characterization of neuwiedase, a nonhemorrhagic fibrin(ogen)olytic metalloprotease from *Bothrops neuwiedi* snake venom. Arch. Biochem. Biophys. 381, 213–224.

Sanchez, E.F., Diniz, C.R., Richardson, M., 1991. The complete amino acid sequence of the hemorrhagic factor LHFII, a metalloproteinase isolated from the venom of the bushmaster snake (Lachesis muta muta). FEBS Lett. 282, 178–182.

Selistre de Araujo, H.S., Ownby, C.L., 1995. Molecular cloning and sequence analysis of cDNAs for metalloproteinases from broad-banded copperhead *Agkistrodon contortrix* laticinctus. Arch. Biochem. Biophys. 320, 141–148.

Siigur, J., Samel, M., Ton¨ismaġi, K., Subbi, J., Siigur, E., Tu, A.T., 1998. Biochemical characterization of lebetase, a direct-acting fibrinolytic enzyme from *Vipera lebetina* snake venom. Tromb. Res. 90, 39–49.

Tu, A.T., Baker, B., Wongvilibulsin, S., Willis, T., 1996. Biochemical characterization of atroxase and nucleotide sequence encoding the fibrinolytic enzyme. Toxicon 34, 1295–1300.

Takeya, H., Onikura, T., Sugihara, H., Iwanaga, S., 1990. Primary structure of a hemorrhagic metalloproteinase, HT-2, isolated from the venom of *Crotalus ruber ruber*. J. Biochem. 108, 711–719.

Watanabe, L., Shannon, J.D., Valente, R.H., Rucavado, A., Alape-Giron, A., Kamiguti, A., Theakston, R.D., Fox, J.W, Gutierrez, J.M., Arni,

R.K., 2003. Amino acid sequence and crystal structure of BaPl, a metalloproteinase from *Bothrops asper* snake venom that exerts multiple tissue-damaging activities. Protein Sci. 12, 2273–2281.

Weissenberg, S., Ovadia, M., Fleminger, G., Kochva, E., 1991. Antihemorrhagic factors from blood serum of the western diamondback rattlesnake Crotalus Atrox. Toxicon 29, 807–818.

Zhang, D., Botos, I., Gomis-Rueth, F.-X., Doll, R., Blood, C., Njoroge, F.G., Fox, J.W., Bode, W., Meyer, E.F., 1994. Structural interaction of natural and synthetic inhibitors with the venom metalloproteinase, atrolysin C (form d). Proc. Natl Acad. Sci. USA 91, 8447–8451.

Zhu, X., Teng, M., Niu, L., 1999. Structure of acutolysin-C, a Hemorrhagic toxin from the venom of *Agkistrondon acutus*, providing further evidence for the mechanism of the pH-dependent proteolytic reaction of zinc metalloproteinases. Acta Crystallogr. D 55, 1834.